APPLICATION OF NONLINEAR CONTROL FOR HARD TRUCK PLATOONING

A Thesis

by

DAVID JOSEPH FRANKLIN

Submitted to the Office of Graduate and Professional Studies of
Texas A&M University
in partial fulfillment of the requirements for the degree of

MASTER OF SCIENCE

Chair of Committee,	Swaminathan Gopalswamy
Committee Members,	Won-Jong Kim
	John Valasek
Head of Department,	Andreas Polycarpou

May 2020

Major Subject: Mechanical Engineering

ABSTRACT

This research describes a novel concept called "Hard Truck Platooning" that achieves platooning between commercial tractor trailers with the aid of a smart tow hitch between the trailer of the leading vehicle and the tractor of the following vehicle. The control of the following vehicle is governed by highly nonlinear dynamics. This project presents a nonlinear control strategy that comprehends such dynamics. First an appropriate set of tracking variables that will satisfy the overall platooning objectives is identified. Then the system dynamics is cast in terms of these tracking variables. An input-output feedback linearization technique is used for the controller to track the reference values for these variables. Simulation results for a two truck platooning experiment are presented to illustrate and validate the developed controller. Lastly, progress is presented on physical implementation of this controller on a pair of semi trucks.

DEDICATION

For my parents and Jesus.

ACKNOWLEDGMENTS

I would like to thank Dr. Sri Saripalli for letting us use his semi truck for our experiments, and Drew Hubbard for driving the truck for us. I would like to thank Dr. Beth Deuermeyer and Dr. Dennis Perkinson for their support and encouragement at the Aggie Forum, and Mike Ashley for all his help and hard work on this project! I would also like to thank my advisor Dr. Gopalswamy for all his help and support throughout my time at A&M!

CONTRIBUTORS AND FUNDING SOURCES

Contributors

This work was supported by a thesis committee consisting of my advisor Professor Swami Gopalswamy in the mechanical engineering department, Professor Won-Jong Kim in the mechanical engineering department, and Professor John Valasek in the aerospace engineering department.

The prototype hard tow bar was designed and fabricated by a mechanical engineering senior design team of Dylan Freeman, Bryce Himmelreich, Stephen Hunter, Aaron Sanderson, Austin Shay, Hunter Teague, Connor Ughetta, and Hayden Woods. The tow bar was further refined by Mike Ashley, a mechanical engineering senior, who also designed and fabricated parts to attach the tow bar to the semi truck and trailer and assisted with running tests with the trucks.

Drew Hubbard drove one of our semi trucks during our experiment.

All other work conducted for the thesis was completed by the student independently.

Funding Sources

Graduate study was supported by Dr. Gopalswamy.

NOMENCLATURE

AFC	Army Futures Command
CDL	Commercial Driver's License. This is the driver's license that semi truck drivers must have
FEDC	Fischer Engineering Design Center, which is the machine shop in the Zachry building
Hard truck platooning	Platooning between trucks using a mechanical connection that can carry significant loads
HTP	Hard Truck Platooning
$L_f\vec{h}(\vec{x})$	Lie derivative of $\vec{h}(\vec{x})$ with respect to $\vec{f}(\vec{x})$, which is $\frac{\partial \vec{h}}{\partial \vec{x}}\vec{f}(\vec{x})$
RELLIS Campus	The RELLIS campus of Texas A&M, which is a former Air Force base and has many runways that are well-suited for autonomous vehicle testing
ROS	Robot Operating System
Semi-hard truck platooning	Platooning between trucks using a mechanical connection that does not carry significant loads
Soft truck platooning	Platooning between trucks using a wireless connection
SSI	Synchronous Serial Interface, which is a communication protocol used by some encoders
TAMU	Texas A&M University
TTI	Texas A&M Transportation Institute

TABLE OF CONTENTS

Page

LIST OF FIGURES

FIGURE Page

LIST OF TABLES

TABLE Page

1. INTRODUCTION

1.1 Motivation

Autonomous truck platooning holds huge promise for the future, with fuel savings and reduced CO_2 emissions of up to 16% for following vehicles and up to 8% for the leading vehicle, as well as improved safety and reduced driver fatigue[1]. However, several significant challenges must be overcome before widespread autonomous truck platooning can become a reality. Autonomous vehicles such as trucks must have accurate sensors to perceive their surroundings and use robust algorithms to detect potential obstacles, lane markers, and nearby traffic. If the optimal spacing between vehicles in the platoon is not maintained, the potential fuel savings of platooning will not be fully realized [2]. Additionally, current vehicle-to-vehicle communication between trucks in a platoon is based on wireless communication, which introduces potential security vulnerabilities [3]. Also, current autonomous truck platooning technology requires the driver of an autonomous truck to remain alert at all times, ready to take control of the vehicle as soon as something unexpected occurs[4]. This constant alertness of the driver can negate the promised benefit of reduced driver fatigue. Because of these and other challenges, conventional autonomous truck platooning has not yet gained widespread adoption.

Because current challenges with conventional truck platooning prevent the potential benefits of widespread autonomous truck platooning from being fully realized, there is a great motivation to develop a new type of truck platooning that can overcome these obstacles.

1.2 Introduction

This project addresses these challenges through a novel concept that involves tethering the following vehicles to the lead vehicle through a physical hard-connect that will simultaneously facilitate load and information transfer between the vehicles. This concept is called "Hard Truck Plattoning" or HTP. HTP is a new kind of platooning as illustrated in Fig. 1.1. This concept for truck platooning was originally created by Professor Swaminathan Gopalswamy in the mechanical

engineering department of Texas A&M University[5].

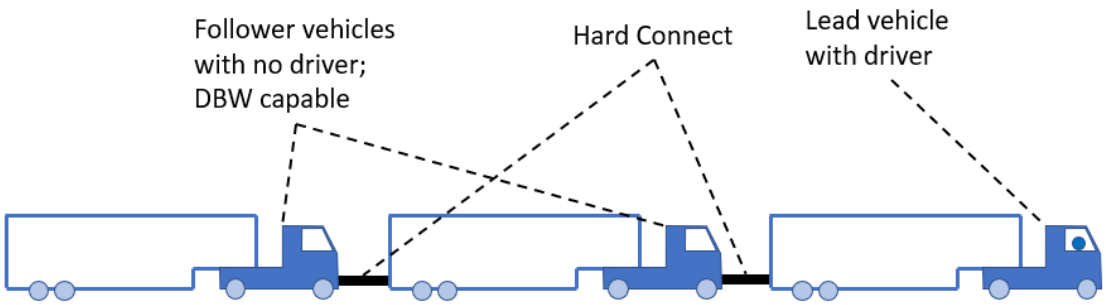

Figure 1.1: HTP Diagram

While this is similar to "towing" one vehicle with another, there are key differences that overcome fundamental limitations of traditional towing methods. In normal towing, the lead vehicle is the primary power source and has to provide the required torque and power to drive the entire platoon. This would require very large engines in the trucks, making them inefficient and bulky. Equally importantly, the hard connection of the platoon vehicles changes the driving dynamics of the platoon dramatically from the driving dynamics of a single vehicle. This makes driving such platoons a very difficult task requiring specialized training. Further, the acceleration and deceleration capabilities of the train become very different from the rest of the traffic, presenting significant safety challenges.

With HTP, the leading truck in the platoon is driven by a human driver, but all of the following trucks are driven autonomously. The front of each following truck is connected to the rear of the trailer in front of it by a "smart" tow bar, or "hard connect." This smart tow bar has a joint at each end and is compliant, so that each truck still has a full range of motion in the plane of the road. These tow bars have sensors to measure their length and the total load on each bar, as well as the acceleration at either end of each bar. The smart hard connects will also transmit information over a wired connection between the trucks. This information, such as the articulation angle of

each joint, the load in each bar, the current length of each bar, and the acceleration of each truck, will inform the control decisions of the following autonomous trucks. Ideally, the control of the following trucks will ensure that each following truck travels through the path set by the leading truck, and that each following truck accelerates and decelerates in sync with the truck in front of it so that the tow bars carry no load.

HTP has several advantages over traditional truck platooning. Because each follower truck is physically linked to the truck in front of it and is following closely behind that truck, the need for obstacle detection, path planning, and obstacle avoidance is reduced. Of course, the following trucks should still be aware of their surroundings, but this is much less safety-critical than it is in conventional autonomous truck platoons. Additionally, the hard connect between each truck helps maintain an ideal gap between each pair of trucks. Because the following trucks are driven autonomously, there is no need for a human driver in them. Because vehicle-to-vehicle communication happens through a wired connection in the tow bar, the HTP method of truck platooning greatly reduces the cyber-security risks associated with conventional truck platooning.

1.3 Technical Challenges

There are several important technical challenges that must be overcome in order to enable HTP. The hard connection must be able to be quickly and easily attached and detached from each vehicle for convenience. The logistics of using this new platooning technology must also be considered. For example, if several truck drivers meet to link together and have one of them drive all the trucks in a platoon, the remaining drivers must arrange for their own transportation now that their trucks are driving away in the platoon. This logistics problem would exacerbated if HTP became widely adopted. Also, an advanced control strategy must be used to control all the following trucks in the platoon. If the following trucks are not controlled well, then they will push or pull on the leading truck and make it difficult to drive. Semi trucks exhibit nonlinear dynamics, so the following trucks will need an advanced control system that can account for such dynamics.

Although there are many technical challenges that must be overcome, this paper will only focus on one of them, namely, developing an advanced control strategy for the following trucks that will

result in acceptable and safe driving dynamics for the platoon. Also, in this paper a platoon of only two trucks, a leader and a follower, will be considered.

1.4 Literature Review

Much research on truck platooning has focused on platooning where the trucks wirelessly sense each other's position in order to maintain an ideal spacing between vehicles [6]. However, there are several other ways to couple the trucks in a platoon. Besides wireless coupling, which is called "soft" coupling, there is also "semi-hard" and "hard" coupling [7]. Semi-hard coupling involves a physical connection between vehicles that does not transfer significant loads and commonly uses a cable. Hard connection, which this project focuses on, involves a physical connection between vehicles that can carry significant loads. Although much less common, there are a few examples of semi-hard and hard platooning. Autonomous Solutions, Inc. has recently developed a product called the "guideline" that enables semi-hard platooning for military applications [8]. Also, the motorhome company Dethleffs recently developed a camper that has an electric motor mounted at each wheel and strain sensors in its tow hitch, so that it can provide torque at its wheels in order to reduce the load on the vehicle it is being towed by [9]. Several academic papers have alternatively used soft[10], semi-hard[11], and hard coupling[12] [13] [14] to create a platoon of small personal electric vehicles to give greater mobility to elderly people in Japan.

1.5 Overview

Section 2 of this paper will present a simplified dynamic model of the semi truck platoon. Section 3 will develop a control strategy for the following semi truck using feedback linearization. Section 4 will show simulation results of the control strategy, and section 5 will describe current progress on implementing this control scheme on real semi trucks. Lastly, section 6 will present a summary and conclusion.

2. DYNAMICS

2.1 Introduction

This section derives a two-dimensional planar dynamic model of an articulated semi truck, based on Gafvert et al's "Truck model for Yaw Dynamics Control"[15]. The truck and trailer will be treated as two distinct rigid bodies that are connected by a pin joint at their hitches. Then Newton's Second Law will be applied to the free-body diagrams of the truck and trailer to derive three equations of motion for the truck and three more equations for the trailer. Because the pin joint at the hitch eliminates two degrees of freedom from the system of two rigid bodies, two of the six equations of motion are redundant and will be eliminated through algebra. The remaining four equations of motion will be recast in terms of the longitudinal velocity of the truck, the lateral velocity of the truck, the yaw rate of the truck, and the articulation angle of the trailer, which is used here to denote the difference between the yaw angle of the truck and the yaw angle of the trailer. Once the equations of motion for a semi truck and trailer have been derived, two systems of a truck and trailer will be combined into one larger dynamic system by finding the forces a smart tow bar would exert on each truck and trailer.

2.2 Assumptions and Limitations

Several simplifying assumptions were made during the derivation of this dynamic model. This is a 2D rigid body dynamic model, so pitch, roll, and vertical motion are all neglected. When the smart tow bar is introduced into the model, it will be modelled as a massless spring since this will simplify the calculations and because the weight of the tow bar is much less than the weight of the semi trucks or trailers. The tow bar is modelled as a spring because making the tow bar complaint will help reduce impact loads and make the platoon safer. The spring force in the tow bar will also be modelled as a linear spring for simplicity. The hitch of the trucks and trailers will be modelled as a frictionless pin joint. This assumption was made to simplify the derivation, because the hitch is thoroughly greased, and because the friction forces at the hitch are expected to be very small

compared with the masses of the truck and trailer as well as the the forces exerted by the truck. For simplicity, this dynamic model does not include aerodynamic forces, rolling resistance, or powertrain dynamics. There are only 6 tire forces modelled in the free body diagram of the truck and trailer, although there are 18 wheels on normal semi trucks and trailers. This is because the groups of 4 tires located on either side at the back of the truck and the back of the trailer have been consolidated into one combined tire force. This simplification was made because the tires in each set of 4 are located very close together. Another simplification is that this dynamic model calculated the lateral tire forces using a linear tire model. This means that the lateral force exerted by each tire is proportional to the slip angle at each tire, which is the angle between the direction the tire is pointing and the velocity vector of the tire. This linear tire model is not valid for large slip angles, so this model is not suitable if the trucks start drifting or sliding out of control, but it is suitable for normal highway driving conditions.

2.3 Rigid Body Dynamics

Fig. 2.1 is a free body diagram showing the forces that act on the truck and trailer. Here the truck and trailer are treated as two distinct rigid bodies which are coupled through the forces at the hitch, which are denoted by X_P and Y_P and are aligned with the longitudinal and lateral axes of the truck.

The forces X_1, X_2, X_3, and X_4 are the longitudinal tire forces acting on the truck while Y_1, Y_2, Y_3, and Y_4 are the lateral tire forces acting on the truck. Likewise, the forces X_5 and X_6 are the longitudinal tire forces acting on the trailer, while Y_5 and Y_6 are the lateral tire forces acting on the trailer. Although semi trucks commonly have two rear axles with four tires on each axle, the truck in this derivation is modelled as having one rear axle with two tires because the tire forces from the four rear tires on each side of the truck can be grouped together and treated as one combined tire force. The tires at the rear of the trailer are combined similarly.

Newton's Second Law can be applied to the free body diagram in Fig. 2.1 to solve for the acceleration of the center of mass of the truck. Equations (2.1) and (2.2) below are equations of motion for the longitudinal and lateral acceleration of the truck. The subscript 1 indicates that

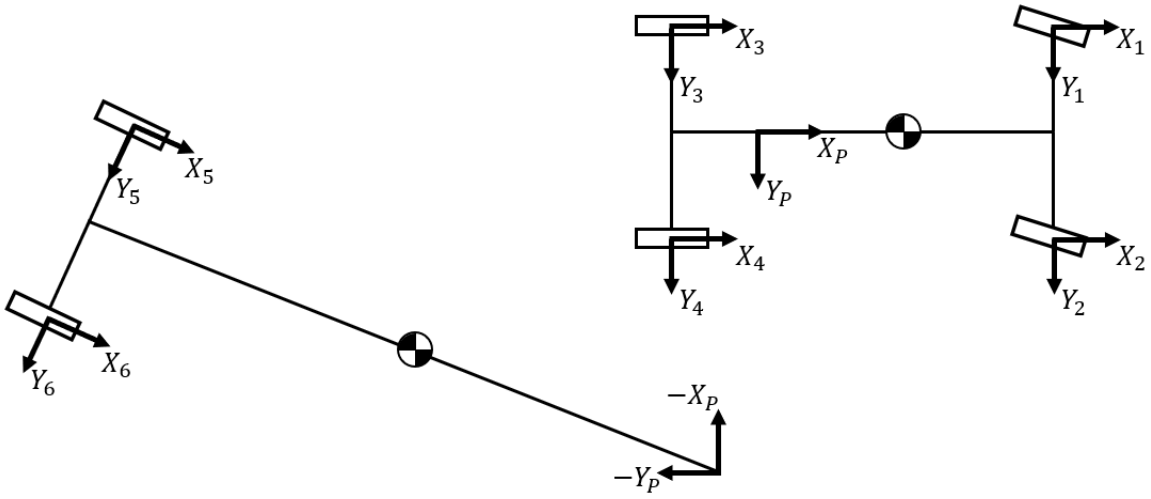

Figure 2.1: Free Body Diagrams of the Truck and Trailer

the term is associated with the lead truck and trailer, while the subscript 2 indicates that the term is associated with the following truck and trailer. Also, the subscript v shows that the term is associated with the vehicle, which is the truck, and the subscript t shows that the term is associated with the trailer. Table 2.1 shows the meaning of different variables used in this system.

$$m_v \left(\dot{U}_v - r_v^2 d_v - r_v V_v \right) = \bar{X}_v + X_P \tag{2.1}$$

$$m_v \left(\dot{V}_v + \dot{r}_v d_v + r_v U_v \right) = \bar{Y}_v + Y_P \tag{2.2}$$

The same procedure can be followed for the trailer to produce Equations (2.3) and (2.4), which are equations of motion for the lateral and longitudinal acceleration of the trailer.

$$m_t \left(\dot{U}_t + r_t^2 d_t - r_t V_t \right) = \bar{X}_t - X_P \cos\psi - Y_P \sin\psi \tag{2.3}$$

$$m_t \left(\dot{V}_t - \dot{r}_t d_t + r_t U_t \right) = \bar{Y}_t + X_P \sin\psi - Y_P \cos\psi \tag{2.4}$$

The sum of the moments about the hitch of the truck and trailer can be taken to yield Equations (2.5) and (2.6) below for the angular acceleration of the truck and trailer.

Table 2.1: Nomenclature

Term	Description
d_v	distance from truck center of mass to hitch
d_t	distance from trailer center of mass to hitch
m_v	mass of the truck
m_t	mass of the trailer
x	truck hitch global x coordinate
y	truck hitch global y coordinate
U	truck longitudinal velocity
V	truck lateral velocity
$\dot{U}$	longitudinal acceleration of the truck
$\dot{V}$	lateral acceleration of the truck
θ	global yaw angle of the truck
ψ	articulation angle of trailer
r	yaw rate of the truck
$\dot{r}$	angular acceleration of the truck
$\bar{X}_v$	sum of the forces X_1, X_2, X_3, and X_4
$\bar{Y}_v$	sum of the forces Y_1, Y_2, Y_3, and Y_4
$\bar{X}_t$	sum of the forces X_5 and X_6
$\bar{Y}_t$	sum of the forces Y_5 and Y_6
$\bar{Z}_v$	sum of external moments acting on the truck
$\bar{Z}_t$	the sum of the external moments acting on the trailer
I_v	moment of inertia of the truck about its hitch
I_t	moment of inertia of the trailer about its hitch

$$I_v\dot{r}_v + m_v d_v \left(\dot{V}_v + U_v r_v\right) = \bar{Z}_v \tag{2.5}$$

$$I_t\dot{r}_t - m_t d_t \left(\dot{V}_t + U_t r_t\right) = \bar{Z}_t \tag{2.6}$$

These six coupled equations are the equations of motion of the truck and trailer. The six state variables in the coupled equations of motion are the longitudinal, lateral, and angular velocities of the truck and trailer: U_v, V_v, r_v, U_t, V_t, and r_t. There are six equations because there are three equations of motion for each rigid body. However, because the bodies are connected by a pin joint at the hitch, there are only four degrees of freedom in the system, so two equations of motion are redundant and can be eliminated through algebra. For convenience, the variables U_t and V_t will be

eliminated, and r_t will be replaced by ψ, the articulation angle between the truck and trailer, which is the angle between the longitudinal axis of the truck and that of the trailer.

Completing this algebra to eliminate variables results in Equations (2.7), (2.8), and (2.9) below.

$$\begin{aligned} I_t\left(\ddot{\psi}+\dot{r}_v\right) - m_t d_t\Big(\left(\dot{V}_v + U_v r_v\right)\cos\psi \\ -\left(\dot{U}_v - V_v r_v\right)\sin\psi\Big) = \bar{Z}_t \end{aligned} \tag{2.7}$$

$$\begin{aligned} \left(m_v+m_t\right)\left(\dot{V}_v+U_v r_v\right) + m_v\dot{r}_v d_v + \\ m_t d_t\left(\dot{\psi}+r_v\right)^2\sin\psi - \left(\ddot{\psi}+\dot{r}_v\right)m_t d_t\cos\psi \\ = \bar{Y}_v + \bar{X}_t\sin\psi + \bar{Y}_t\cos\psi \end{aligned} \tag{2.8}$$

$$\begin{aligned} \left(m_v+m_t\right)\left(\dot{U}_v - r_v V_v\right) - m_v r_v^2 d_v + \\ \left(\dot{\psi}+r_v\right)^2 d_t m_t\cos\psi + \left(\ddot{\psi}+\dot{r}_v\right)d_t m_t\sin\psi \\ = \bar{X}_v + \bar{X}_t\cos\psi - \bar{Y}_t\sin\psi \end{aligned} \tag{2.9}$$

Equations (2.5), (2.7), (2.8), and (2.9) are the main four equations of motion of the system, where the main state variables are U_v, V_v, r_v, ψ, and $\dot{\psi}_v$. These state variables are expressed together, along with a few other state variables for convenience, in a state vector $\vec{\zeta}$ in Equation (2.10) below.

$$\vec{\zeta} = \Big[U_v, V_v, r_v, \dot{\psi}, \psi, \theta, x_v, y_v\Big]^\top \tag{2.10}$$

The equations of motion are coupled and implicit, so they will be expressed in the following matrix form, where $M(\vec{\zeta})$ is the mass matrix, which is a function of $\vec{\zeta}$, and $\vec{f}(\vec{\zeta})$ is the forcing function vector, which is also a function of $\vec{\zeta}$.

$$M\left(\vec{\zeta}\right)\dot{\vec{\zeta}} = \vec{F}\left(\vec{\zeta}\right) \tag{2.11}$$

Equation (2.12) below shows the mass matrix $M(\vec{\zeta})$. For brevity, several abbreviations are used in the following equation. The total mass of the truck and trailer, which is $m_v + m_t$, is expressed as m, q_1 stands for $m_t d_t \sin\psi$, and q_2 stands for $m_t d_t \cos\psi$.

$$M(\vec{\zeta}) = \begin{bmatrix} m & 0 & q_1 & q_1 & 0 & 0 & 0 & 0 \\ 0 & m & (m_v d_v - q_2) & -q_2 & 0 & 0 & 0 & 0 \\ 0 & m_v d_v & I_v & 0 & 0 & 0 & 0 & 0 \\ q_1 & -q_2 & I_t & I_t & 0 & 0 & 0 & 0 \\ 0 & 0 & 0 & 0 & 1 & 0 & 0 & 0 \\ 0 & 0 & 0 & 0 & 0 & 1 & 0 & 0 \\ 0 & 0 & 0 & 0 & 0 & 0 & 1 & 0 \\ 0 & 0 & 0 & 0 & 0 & 0 & 0 & 1 \end{bmatrix} \tag{2.12}$$

Equation (2.13) below describes the forcing function $\vec{f}(\vec{\zeta})$, with several abbreviations for convenience.

$$
\begin{aligned}
F_1 = mr_v V_v - m_t d_t \left(\dot{\psi} + r_v\right)^2 \cos(\psi) + \\
m_v r_v^2 d_v + \bar{X}_v + \bar{X}_t \cos\psi - \bar{Y}_t \sin\psi \\
F_2 = -mU_v r_v - m_t d_t \left(\dot{\psi} + r_v\right)^2 \sin\psi + \\
\bar{Y}_v + \bar{X}_t \sin\psi + \bar{Y}_t \cos\psi
\end{aligned}
$$

$$
\vec{f}(\vec{\zeta}) = \begin{bmatrix}
F_1 \\
F_2 \\
-m_v d_v U_v r_v + \bar{Z}_v \\
m_t d_t r_v \left(U_v \cos\psi + V_v \sin\psi\right) + \bar{Z}_t \\
\dot{\psi} \\
r \\
U\cos\theta - V\sin\theta \\
-U\sin\theta - V\cos\theta
\end{bmatrix} \tag{2.13}
$$

The matrix $M(\vec{\zeta})$ is invertible, so the equations of motion could be expressed in an explicit form instead of an implicit form, but the resulting explicit equations would be very long and cumbersome, so it is much more convenient to express the equations of motion their current form. Interested readers should see the appendix for an explanation why the mass matrix is invertible.

As mentioned earlier, the lateral tire forces are found through the use of a simple linear tire model, in which the lateral force on the vehicle is proportional to the slip angle of the tire. The slip angle of the tire is the angle between the direction the tire is pointing and the velocity vector of the tire.

In this simplified model, rolling resistance is neglected, so the longitudinal tire forces at the wheels that are not driven are zero. This model assumes that the truck is a rear-wheel drive truck, which means that X_1, X_2, X_5, and X_6 are all zero. This model does not consider powertrain dynamics of the truck, so the longitudinal force at each of the drive wheels, X_3 and X_4, are treated

as inputs, with each of them providing a throttle force τ.

Now that the forces at each tire are defined, the equations of motion for one semi truck and trailer are completed. The linear tire model is only valid for small slip angles, but no other small angle assumptions were used when deriving this model. This model can be extended by considering a platoon of two semi trucks, with the follower truck connected to the leading trailer by a tow bar.

2.4 Combining Trucks into One System

Now the equations of motion for two semi trucks and trailers will be combined into one larger system. Equation (2.14) shows the state vectors for both the leading and following systems.

$$\begin{aligned} \vec{\zeta_1} &= \begin{bmatrix} U_1, V_1, r_1, \dot{\psi}_1, \psi_1, \theta_1, x_1, y_1 \end{bmatrix}^\top \\ \vec{\zeta_2} &= \begin{bmatrix} U_2, V_2, r_2, \dot{\psi}_2, \psi_2, \theta_2, x_2, y_2 \end{bmatrix}^\top \end{aligned} \tag{2.14}$$

Because the lead truck is driven by a person and the following truck is driven autonomously, the throttle and steering angle of the following truck are treated as control inputs to the system. Equation (2.15) below shows the input vector $\vec{u}$, where τ_2 is the throttle force for the rear truck and δ_2 is the steering angle for the following truck.

$$\vec{u} = \begin{bmatrix} \tau_2 \\ \delta_2 \end{bmatrix} \tag{2.15}$$

Equation (2.16) below shows an abbreviated form of the equations of motion for each separate truck and trailer, which were developed earlier, to emphasize that the control input $\vec{u}$ affects the following system. In these equations of motion, $M(\vec{\zeta})$ is the mass matrix of each system and $\vec{f}(\vec{\zeta})$ is the forcing function of each system.

$$\begin{aligned} M_1\left(\vec{\zeta_1}\right)\dot{\vec{\zeta_1}} &= \vec{f_1}\left(\vec{\zeta_1}\right) \\ M_2\left(\vec{\zeta_2}\right)\dot{\vec{\zeta_2}} &= \vec{f_2}\left(\vec{\zeta_2}, \vec{u}\right) \end{aligned} \tag{2.16}$$

To consider the entire platoon as one system, both state vectors can be concatenated into one combined state vector, $\vec{x}$, as shown in Equation (2.17).

$$\vec{x} = \begin{bmatrix} \vec{\zeta_1} \\ \vec{\zeta_2} \end{bmatrix} \tag{2.17}$$

Likewise, the equations of motion in Equation (2.16) can be combined to form the combined equation of motion in Equation (2.18) below.

$$M_c\left(\vec{x}\right)\dot{\vec{x}} = \vec{f_c}\left(\vec{x}, \vec{u}\right) \tag{2.18}$$

Inverting the $M_c(\vec{x})$ matrix in Equation (2.18) produces Equation (2.19) below. The combined mass matrix $M_c(\vec{x})$ is a block diagonal matrix, composed of an upper block $M_1(\vec{\zeta_1})$ and a lower block $M_2(\vec{\zeta_2})$. Because both these blocks are invertible, as mentioned earlier, the block diagonal matrix $M_c(\vec{x})$ is also invertible.

$$\dot{\vec{x}} = \vec{f}\left(\vec{x}\right) + \vec{g}\left(\vec{x}, \vec{u}\right) \tag{2.19}$$

The function $\vec{g}\left(\vec{x}, \vec{u}\right)$ is linear with respect to the input vector $\vec{u}$, so Equation (2.19) reduces to Equation (2.20) below.

$$\dot{\vec{x}} = \vec{f}\left(\vec{x}\right) + g\left(\vec{x}\right)\vec{u} \tag{2.20}$$

2.5 Finding Tow Bar Forces

Now that the equations of motion for both the leader and follower systems have been combined, the tow bar forces linking them together can be found. Fig. 2.2 below shows two semi trucks connected by a tow bar. The small rectangles represent semi trucks, the long rectangles represent the trailers, and the dark line in the middle depicts the tow bar. The diagram labels several different angles on the platoon.

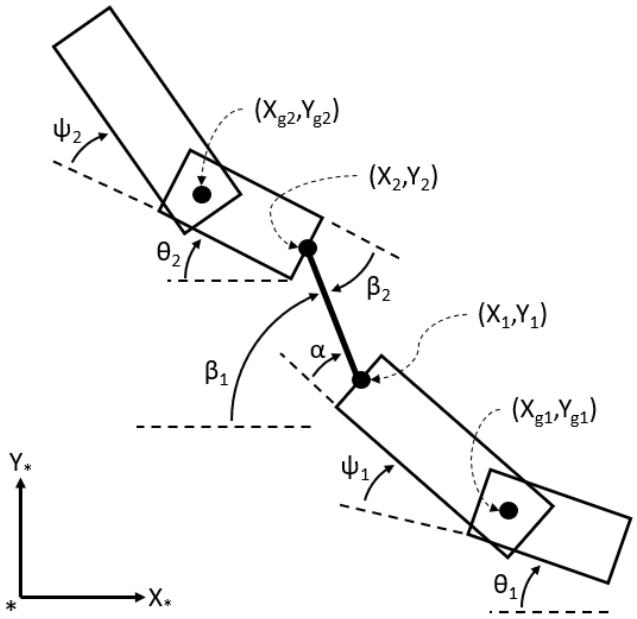

Figure 2.2: Diagram a Semi Truck Platoon

The tow bar will exert forces on the rear of the leading trailer and on the front of the following truck. Fig. 2.3 below is a diagram showing these forces from the tow bar acting on a truck and trailer. The forces X_{tv} and Y_{tv} are the longitudinal and lateral forces that act on the front of the truck, and X_{tt} and Y_{tt} are the forces that act on the rear of the trailer. If there are only two trucks in the platoon, then the forces X_{tv} and Y_{tv} will be zero for the leading truck and trailer, while the forces X_{tt} and Y_{tt} will be zero for the following trailer.

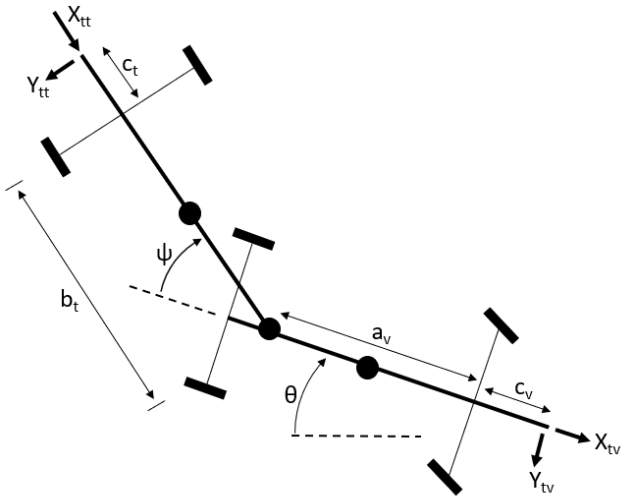

Figure 2.3: Diagram of Forces from the Tow Bar

This figure introduces two new dimensions on the truck and trailer. The distance c_v is the distance between the truck's front axle and the point where the tow bar connects to the front of the truck and causes the forces X_{tv} and Y_{tv}. Similarly, the distance c_t is the distance between the rear axle of the trailer and the point where the tow bar connects to the rear of the trailer and causes the forces X_{tt} and Y_{tt}.

The tow bar is modelled as a spring, connected to the rear of the leading trailer and the front of the following truck with pin joints. Equation (2.21) illustrates this, where F is the total compressive force in the tow bar, k is the spring constant of the tow bar, l_0 is the initial uncompressed length of the tow bar, and l is the current length of the tow bar. In simulations, F can be calculated this way, though in real experiments F would be measured directly.

$$F = k\,(l_0 - l) \tag{2.21}$$

Because the tow bar is connected by pin joints at both ends, it is a two-force member and only transmits forces that are aligned with the tow bar. Based on this information, the forces X_{tv}, Y_{tv}, X_{tt}, and Y_{tt} can be solved for in terms of F and the angles labeled in Fig 2.2. Here X_{tv} and Y_{tv}

refer to the forces acting at the front of the following truck while X_{tt} and Y_{tt} refer to the forces acting at the rear of the leading trailer. Equation (2.22) below shows expressions for these forces.

$$\begin{aligned} X_{tv} &= -F\cos\beta_2 \\ Y_{tv} &= -F\sin\beta_2 \\ X_{tt} &= F\cos\alpha \\ Y_{tt} &= F\sin\alpha \end{aligned} \tag{2.22}$$

Equation (2.23) shows how to solve for l, the length of the tow bar, from x_1, y_1, x_2, and y_2, as depicted in Fig. 2.2. In simulations, l can be calculated this way, though in physical experiments l can be measured directly.

$$l = \sqrt{(x_1 - x_2)^2 + (y_1 - y_2)^2} \tag{2.23}$$

Now that the forces in Equation (2.22) have been defined, they can easily be included in the equations of motion of the trucks and trailers. This is done by treating them as external forces, similar to tire forces, and including them in the $\bar{X}$, $\bar{Y}$, and $\bar{Z}$ terms.

Fig. 2.4 shows a diagram of the leading trailer and following truck connected by the tow bar. This figure labels the points (x_1, y_1) and (x_2, y_2) as well as the length of the tow bar l and the angle between the tow bar and the longitudinal axis of the leading trailer α.

The terms α and Δl are defined in Equation (2.24) below, where l_0 is the original uncompressed length of the tow bar. Again, in simulations Δl and α and be calculated this way, but in real experiments they would be measured more directly. As shown in Fig 2.4, α is the angle between the tow bar and the longitudinal axis of the leading trailer, and Δl is the change in length of the tow bar.

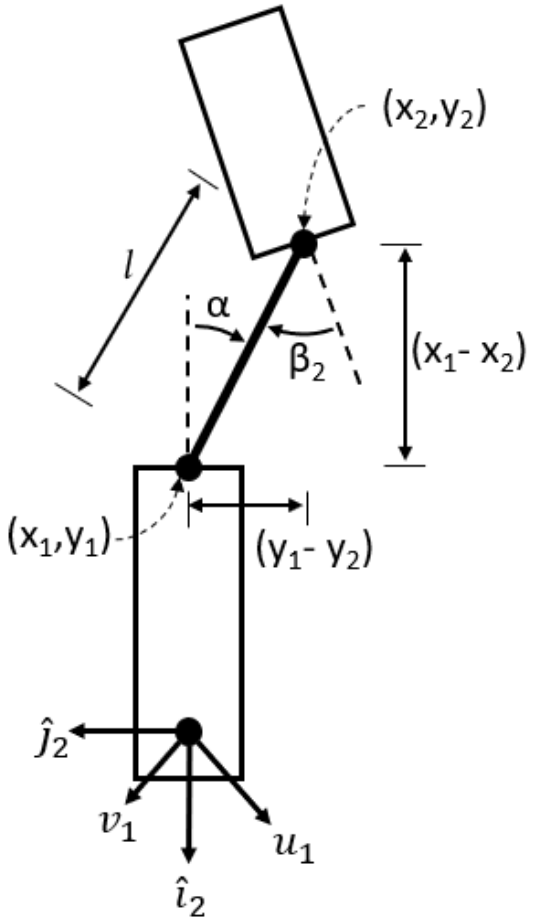

Figure 2.4: Diagram of Dimensions of the Tow Bar

$$\begin{aligned} \Delta l &= l_0 - \sqrt{(x_1 - x_2)^2 + (y_1 - y_2)^2} \\ \alpha &= \arctan\left(\frac{y_1 - y_2}{x_1 - x_2}\right) \end{aligned} \tag{2.24}$$

The terms α and Δl will be treated as measured outputs of the system and combined into the output vector $\vec{y}$ as shown in Equation (2.25) below.

$$\vec{y} = \begin{bmatrix} \Delta l \\ \alpha \end{bmatrix} \tag{2.25}$$

Equations (2.24) and (2.25) are summarized in Equation (2.26) below.

$$\vec{y} = \vec{h}\left(\vec{x}\right) \tag{2.26}$$

3. CONTROLS

3.1 Introduction

The goal of the HTP control system is to make the lead driver feel that he is just driving his own truck. This means that the dynamics of the platoon should effectively reduce to the dynamics of the lead truck. Feedback linearization is a nonlinear control technique used to cancel out unwanted nonlinear dynamics and substitute in desired stable dynamics, so this technique will be used in this project.

In order for the lead driver feel as if he is just driving his own truck, the follower trucks must not push or pull on his truck through the tow bar forces. Because of this, one control objective will be to minimize the tow bar forces. Because the tow bar is modelled as a spring, another way to express this objective is to minimize Δl, which is the change in length of the tow bar and is one of the outputs.

Another goal of the HTP control system is to make the follower trucks travel through the same path that the lead truck took. Because of this, another control objective will be to minimize α, which is the angle between the tow bar and the longitudinal axis of the leading trailer. The angle α is also one of the chosen outputs. This control objective was chosen because if α is zero, then the follower truck will follow directly behind the lead trailer.

This paper uses feedback linearization to control the following semi truck. The high-level procedure to use feedback linearization is to differentiate the output equation until the the input vector appears in the equation. Then a new term $\vec{S}$ is defined in terms of the output and its derivatives such that if $\vec{S}$ goes to zero, then the output will go to zero as well. Finally, the differentiated output equation is substituted into the equation for $\vec{S}$ and the input vector is solved for. By using this strategy to find the input vector, $\vec{S}$ will go to zero, which will cause the output vector to go to zero as well.

There are many ways to define the vector $\vec{S}$ to make both it and $\vec{y}$ go toward zero, but here $\vec{S}$ is

defined so both it and $\vec{y}$ have first order dynamics. First order dynamics were chosen for simplicity and to reduce the number of tuning parameters in the controller.

Since the output equation Equation (2.26) does not include the control input vector $\vec{u}$, the equation must be differentiated with respect to time repeatedly until the input vector appears.

3.2 Finding Derivatives

Differentiating Equation (2.26) with respect to time yields Equation (3.1) below. Please note that the term $L_f\vec{h}(\vec{x})$ is the "Lie Derivative" of $\vec{h}(\vec{x})$ with respect to $\vec{f}(\vec{x})$ and is equivalent to $\frac{\partial \vec{h}}{\partial \vec{x}}\vec{f}(\vec{x})$ as noted in the nomenclature page at the beginning of this paper.

$$\dot{\vec{y}} = L_f\vec{h}\,(\vec{x}) \tag{3.1}$$

The input vector does not appear in Equation (3.1) so the equation will be differentiated with respect to time again, which results in Equation (3.2).

$$\ddot{\vec{y}} = L_f L_f\vec{h}\,(\vec{x}) + L_g L_f\vec{h}(\vec{x})\vec{u} \tag{3.2}$$

The input vector $\vec{u}$ appears in Equation (3.2) so there is no need to further differentiate the equation. For convenience, Equation (3.2) will be abbreviated to Equation (3.3) below. Please note that in Equation (3.3), $\ddot{\vec{y}}$ is linear with respect to $\vec{u}$, which means that this is an affine system.

$$\ddot{\vec{y}} = \vec{c}\,(\vec{x}) + J\,(\vec{x})\,\vec{u} \tag{3.3}$$

Equations (3.1), (3.2), and (3.3) express the equations in very general terms, but the following steps explain the process and equations in more detail. The second derivative of Δl will be found, and then the second derivative of α will be found afterward.

Equation (3.4) shows several relationships based on the angles and points in Fig. 2.4 that will help simplify the controller equations.

$$\begin{aligned} x_1 - x_2 &= l\cos\alpha \\ y_1 - y_2 &= l\sin\alpha \end{aligned} \tag{3.4}$$

Taking the second derivative of Equation (2.23) with respect to time and substituting in Equation (3.4) along with its derivatives with respect to time results in Equation (3.5).

$$\ddot{\Delta}l = -\left(\ddot{x}_1\cos\alpha + \ddot{y}_1\sin\alpha\right) + \left(\ddot{x}_2\cos\alpha + \ddot{y}_2\sin\alpha\right) - l\dot{\alpha} \tag{3.5}$$

This equation includes terms such as $\ddot{x}_1$, $\ddot{y}_1$, $\ddot{x}_2$, and $\ddot{y}_2$, which denote the acceleration of the points (x_1, y_1) and (x_2, y_2) in the local reference frame of the leading trailer. In real experiments, the acceleration of the point (x_1, y_1) can be measured by accelerometers or calculated in terms of other measured quantities, but in simulations this quantity must be calculated in terms of the state variables. Also, the terms $\ddot{x}_2$, and $\ddot{y}_2$, which denote the acceleration of the point (x_2, y_2), must be expanded to a form which includes the inputs τ_2 and δ_2 for the rear truck.

Equation (3.6) shows an expression for the acceleration of the point (x_2, y_2) in the local reference frame of the following truck. In this equation, $\dot{U}_{2v}$ and $\dot{V}_{2v}$ are the longitudinal and lateral accelerations of the hitch of the following truck, U_{2v} and V_{2v} are the longitudinal and lateral velocities of the following truck, $\dot{r}_{2v}$ is the angular acceleration of the following truck, and r_{2v} is the angular velocity of the following truck.

$$\begin{aligned} \ddot{x}_2 &= \dot{U}_{2v} - r_{2v}^2\left(a_v + c_v\right) - r_{2v}V_{2v} \\ \ddot{y}_2 &= \dot{V}_{2v} + \dot{r_{2v}}\left(a_v + c_v\right) + r_{2v}U_{2v} \end{aligned} \tag{3.6}$$

This equation gives the acceleration of the point (x_2, y_2) in the local frame of the following truck, but this acceleration needs to be in the local frame of the leading trailer, since the terms $\ddot{x}_1$ and $\ddot{y}_1$ are in the frame of the leading trailer, and both accelerations need to be in the same

reference frame if they are to be subtracted from each other.

The terms $\dot{U}_{2v}$ and $\dot{V}_{2v}$ in Equation (3.6) are the longitudinal and lateral accelerations of the hitch of the following truck, in the local reference frame of the following truck. These terms were found implicitly in Equation (2.11), but they are needed explicitly in Equation (3.6). Because of this, Equation (2.11) will be solved for $\dot{\vec{\zeta}}$, by inverting the matrix $M(\vec{\zeta})$ as shown in Equation (3.7).

$$\dot{\vec{\zeta}} = M(\vec{\zeta})^{-1} F(\vec{\zeta}) \tag{3.7}$$

Fortunately, the matrix $M(\vec{\zeta})$ is invertible so $\dot{\vec{\zeta}}$ can be found explicitly, but the expression for some elements of the vector $\dot{\vec{\zeta}}$ is thousands of characters long, so the full explicit expression of $\dot{\vec{\zeta}}$ is not included here. An abbreviated explicit form of selected elements of $\dot{\vec{\zeta}}$ is shown in Equation (3.8) below.

$$\begin{aligned} \dot{V}_{2v} &= A(\psi_2)\delta_2 + B(\psi_2)\tau_2 + C(\vec{\zeta}) \\ \dot{U}_{2v} &= D(\psi_2)\delta_2 + E(\psi_2)\tau_2 + F(\vec{\zeta}) \\ \dot{r}_{2v} &= G(\psi_2)\delta_2 + H(\psi_2)\tau_2 + I(\vec{\zeta}) \end{aligned} \tag{3.8}$$

In Equation (3.8), the terms $A(\psi_2)$, $B(\psi_2)$, $D(\psi_2)$, $E(\psi_2)$, $G(\psi_2)$, and $H(\psi_2)$ are nonlinear functions of only the following trailer articulation angle ψ_2 and various geometric constants and dimensions of the truck and trailer. The terms $C(\vec{\zeta})$, $F(\vec{\zeta})$, and $I(\vec{\zeta})$ are nonlinear functions of the state vector $\vec{\zeta}$, but are not functions of the inputs δ_2 or τ_2. This explicit form of $\dot{V}_{2v}$, $\dot{U}_{2v}$, and $\dot{r}_{2v}$ in Equation (3.8) is very convenient, since each term on the left hand side is a linear function of the inputs δ_2 and τ_2, and since the coefficients of the inputs, although nonlinear, are only functions of the trailer articulation angle ψ_2.

Substituting Equation (3.8) into the rotated version of Equation (3.6), and substituting the resulting equation, along with expressions for $\ddot{x}_1$ and $\ddot{y}_1$, into Equation (3.5) results in Equation (3.9) below, where $\overline{A}$, $\overline{B}$, and $\overline{C}$ are defined in Equation (3.10).

This equation has three main terms: δ_2 and its coefficient, τ_2 and its coefficient, and the last term, which is not a function of either input. In this way, the second time derivative of the change in length of the tow bar is a linear function of the inputs δ_2 and τ_2, and the coefficients of the inputs are only functions of the angles ψ_2 and β_2.

$$\ddot{\Delta} l = \overline{A}\left(\psi_2, \beta_2\right) \delta_2 + \overline{B}\left(\psi_2, \beta_2\right) \tau_2 + \overline{C} \tag{3.9}$$

Equation (3.10) is shown below to explain the abbreviating terms in Equation (3.9). Equation (3.10) groups many different terms under the variables of $\overline{A}$, $\overline{B}$, and $\overline{C}$, but it is important to note that $\overline{A}$ and $\overline{B}$ are functions of only the angles ψ_2 and β_2, while $\overline{C}$ depends on many different states and variables. The terms $\bar{c}_1$ and $\bar{c}_2$ are functions of different states and variables, but do not depend on the inputs δ_2 or τ_2.

$$\begin{aligned}
\overline{A}\left(\psi_2, \beta_2\right) &= D\cos(\beta_2) + A\sin(\beta_2) + G\sin(\beta_2)(a_v + c_v) \\
\overline{B}\left(\psi_2, \beta_2\right) &= E\cos(\beta_2) + B\sin(\beta_2) + H\sin(\beta_2)(a_v + c_v) \\
\overline{C} &= F\cos(\beta_2) + C\sin(\beta_2) + I\sin(\beta_2)(a_v + c_v) \\
&\quad + \bar{c}_1\cos(\alpha) + \bar{c}_2\sin(\alpha) - \ddot{x}_1\cos(\alpha) \\
&\quad - \ddot{y}_1\sin(\alpha) - l\dot{\alpha}^2
\end{aligned} \tag{3.10}$$

Equation (3.9) shows a tidy equation for the second time derivative of Δl, which is the change in length of the tow bar, and shows that $\ddot{\Delta} l$ is a linear function of the inputs τ_2 and δ_2. A similar procedure will now be followed to arrive at a similar equation for $\ddot{\alpha}$, which is the second time derivative of the angle between the tow bar and the longitudinal axis of the leading trailer. Once again, Δl and α are the two quantities that this controller is striving to minimize.

Just as was done for the variable Δl, the derivative of α will be taken with respect to time until the inputs δ_2 and τ_2 appear in the expression. This procedure results in Equation (3.11) below.

$$\ddot{\alpha} = -\frac{2\dot{l}\dot{\alpha} - (\ddot{y}_1 - \ddot{y}_2)\cos(\alpha) + (\ddot{x}_1 - \ddot{x}_2)\sin(\alpha)}{l} \tag{3.11}$$

Following the same procedure that was followed for $\ddot{\Delta}l$ and substituting in for $\ddot{x}_2$, $\ddot{y}_2$ using Equations (3.6) and (3.8) achieves the result presented in Equations (3.12) and (3.13)

$$\ddot{\alpha} = \overline{D}\left(\psi_2, \beta_2\right)\delta_2 + \overline{E}\left(\psi_2, \beta_2\right)\tau_2 + \overline{F} \tag{3.12}$$

$$\begin{aligned}
\overline{D}\left(\psi_2, \beta_2\right) &= \frac{-A\cos(\beta_2) + D\sin(\beta_2) - G\cos(\beta_2)(a_v + c_v)}{l} \\
\overline{E}\left(\psi_2, \beta_2\right) &= \frac{-B\cos(\beta_2) + E\sin(\beta_2) - H\cos(\beta_2)(a_v + c_v)}{l} \\
\overline{F} &= \Big(F\sin(\beta_2) - C\cos(\beta_2) - \overline{c}_2\cos(\alpha) \\
&\quad + \overline{c}_1\sin(\alpha) - I\cos(\beta_2)(a_v + c_v) - 2\dot{l}\dot{\alpha} \\
&\quad + \ddot{y}_1\cos(\alpha) - \ddot{x}_1\sin(\alpha)\Big)/l
\end{aligned} \tag{3.13}$$

Now Equations (3.9) and (3.12) can be combined into the matrix equation shown in Equation (3.14).

$$\begin{bmatrix} \ddot{\Delta}l \\ \ddot{\alpha} \end{bmatrix} = \begin{bmatrix} \overline{A} & \overline{B} \\ \overline{D} & \overline{E} \end{bmatrix} \begin{bmatrix} \delta_2 \\ \tau_2 \end{bmatrix} + \begin{bmatrix} \overline{C} \\ \overline{F} \end{bmatrix} \tag{3.14}$$

This equation is the more detailed form of Equation (3.3). Equation (3.15) shows which terms are equivalent between Equation (3.3) and Equation (3.14).

$$\vec{c}(\vec{x}) = \begin{bmatrix} \overline{C} \\ \overline{F} \end{bmatrix}$$
$$J(\vec{x}) = \begin{bmatrix} \overline{A} & \overline{B} \\ \overline{D} & \overline{E} \end{bmatrix} \tag{3.15}$$

3.3 Feedback Linearization

Now that an equation has been found that relates the derivatives of the output vector, $\vec{\dot{y}}$ to the input vector $\vec{u}$, the next step of the control strategy can be carried out.

Equation (3.16) defines a new term $\vec{S}$ which will be used to control the output $\vec{y}$. As can be seen in the equation, if $\vec{S}$ goes to zero, then the output $\vec{y}$ must go to zero as well, because it will have first order dynamics with a time constant λ_y. For this reason, the control system will seek to minimize $\vec{S}$. In this equation, λ_y is a diagonal matrix of positive time constants that will serve as tuning parameters.

$$\vec{S} = \vec{\dot{y}} + \lambda_y \vec{y} \tag{3.16}$$

Differentiating Equation (3.16) with respect to time results in Equation (3.17).

$$\vec{\dot{S}} = \vec{\ddot{y}} + \lambda_y \vec{\dot{y}} \tag{3.17}$$

The vector $\vec{S}$ should go to zero, so it is given first order dynamics as well. This is shown in Equation (3.18) below, where λ_s is another diagonal matrix of positive time constants which function as tuning parameters.

$$\vec{\dot{S}} = -\lambda_s \vec{S} \tag{3.18}$$

Equation (3.19) below shows the structure of the matrices λ_1 and λ_2 in more detail.

$$\lambda_y = \begin{bmatrix} \lambda_{y1} & 0 \\ 0 & \lambda_{y2} \end{bmatrix}$$
$$\lambda_s = \begin{bmatrix} \lambda_{s1} & 0 \\ 0 & \lambda_{s2} \end{bmatrix} \tag{3.19}$$

Substituting Equation (3.18) into Equation (3.17) results in Equation (3.20)

$$\ddot{\vec{y}} + \lambda_y \dot{\vec{y}} = -\lambda_s \vec{S} \tag{3.20}$$

Substituting Equations (3.3) and (3.16) into Equation (3.20) produces Equation (3.21) below.

$$\vec{c}(\vec{x}) + J(\vec{x})\,\vec{u} + \lambda_y \dot{\vec{y}} = -\lambda_s \dot{\vec{y}} + \lambda_y \vec{y} \tag{3.21}$$

The matrix J is invertible, so Equation (3.21) can be rearranged to solve for the control input vector $\vec{u}$, as shown in Equation (3.22).

$$\vec{u} = J(\vec{x})^{-1} \left(-\vec{c}(\vec{x}) - \lambda_y \lambda_s \vec{y} - (\lambda_y + \lambda_s)\,\dot{\vec{y}} \right) \tag{3.22}$$

To provide more detail in this equation, Equations (3.15), (2.25), (2.15), and (3.19) can be substituted in to yield Equation (3.23), which is an equivalent, but more detailed, form of Equation (3.22).

$$\begin{bmatrix} \delta_2 \\ \tau_2 \end{bmatrix} = \begin{bmatrix} \overline{A} & \overline{B} \\ \overline{D} & \overline{E} \end{bmatrix}^{-1} \times \left(- \begin{bmatrix} \overline{C} \\ \overline{F} \end{bmatrix} - \begin{bmatrix} \lambda_{y1}\lambda_{s1} & 0 \\ 0 & \lambda_{y2}\lambda_{s2} \end{bmatrix} \begin{bmatrix} y \\ \alpha \end{bmatrix} - \begin{bmatrix} \lambda_{y1} + \lambda_{s1} & 0 \\ 0 & \lambda_{y2} + \lambda_{s2} \end{bmatrix} \begin{bmatrix} \dot{y} \\ \dot{\alpha} \end{bmatrix} \right) \tag{3.23}$$

This is the control strategy that will be used to control the following semi truck.

4. SIMULATION

The control system and platoon dynamics shown earlier in this paper were simulated using Matlab and Simulink. The values of the constants in the dynamic model of the platoon that were used in the simulation are presented below in Table 4.1. The terms C_{af}, C_{ar}, and C_{at} are the lateral tire stiffness coefficients for the front truck tires, rear truck tires, and trailer tires, respectively. These coefficients can be multiplied by the slip angle at each tire to yield the lateral force produced by each tire in the linear tire model. I_v and I_t are the moments of inertia of the truck and the trailer, respectively, about their hitches. The stiffness coefficient of the hard connect is k. The terms b_v and b_t are the distances from the rear axle of the truck and trailer to the hitch, respectively. Most of these values were chosen based on existing literature[16]. The values are meant to be broadly representative of semi trucks and trailers, and are not meant represent a specific truck or trailer.

Table 4.1: Simulation Constants

Constant	Value	Units
m_v	7050	Kg
m_t	23500	Kg
a_v	2.8	m
b_v	0.7	m
d_v	1.8	m
y_f	1	m
y_r	1	m
b_t	14	m
d_t	7	m
y_t	1	m
C_{af}	143330	N
C_{ar}	573320	N
C_{at}	321248	N
I_v	28492	Kg m^2
I_t	1541800	Kg m^2
c_v	0.7	m
c_t	1.5	m
k	180000	N/m

Several different values of the controller tuning parameters λ_y and λ_s, which are the time constants of the new system dynamics, were tried, and the values shown below in Equation (4.1) were found to produce good results.

$$\lambda_y = \begin{bmatrix} 8 & 0 \\ 0 & 4 \end{bmatrix}$$
$$\lambda_s = \begin{bmatrix} 8 & 0 \\ 0 & 4 \end{bmatrix} \tag{4.1}$$

The first simulation performed shows the behavior of the platoon if the leading truck is driving straight ahead with a constant throttle force of 1000 Newtons and an initial speed of 5 meters per second. The following truck is also given an initial speed of 5 meters per second, but it has an initial trailer articulation angle of -2 degrees, an initial yaw angle of 4 degrees, and an initial horizontal offset of 0.8 meters to the left of the leading truck, so that the tow bar is initially stretched by 4.7 centimeters. This simulation was performed to demonstrate the stability of the controller for simple paths of the leading truck and small initial displacements away from the desired trajectory. The simulation ran for 5 seconds.

Fig. 4.1 shows how the compression in the tow bar, Δl, was driven to zero by the controller. Similarly, Fig. 4.2 shows how the angle between the tow bar and the longitudinal axis of the leading trailer, α, was also driven to zero.

These graphs show that the controller performed well when the lead truck drove straight ahead and the follower truck had small initial conditions, achieving both control objectives by driving Δl and α to zero in a quick but smooth manner.

The controller was tested again in different circumstances, in which the lead truck drove in a circle with a constant steering angle of 3.5 degrees. Both trucks had the same initial conditions, and the lead truck still had a constant throttle input of 1000 Newtons. This simulation was run for 20 seconds.

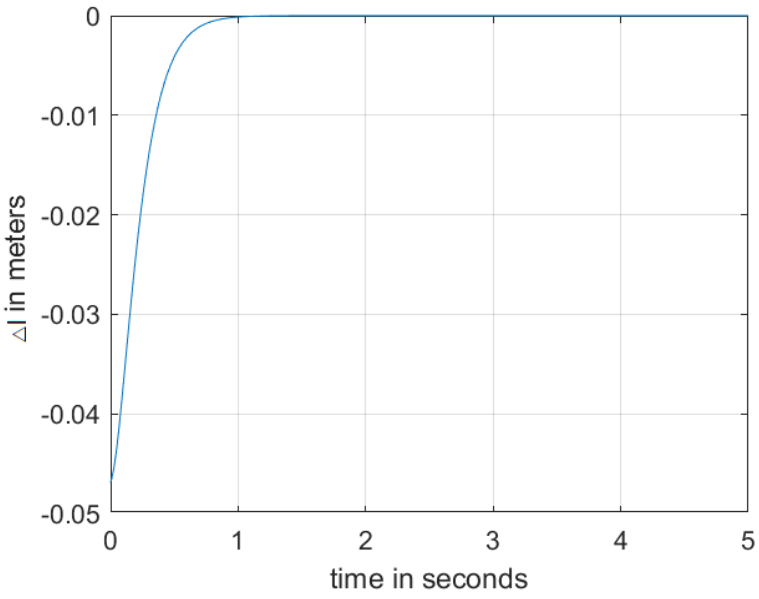

Figure 4.1: Value of Δl as the Platoon Drives Straight

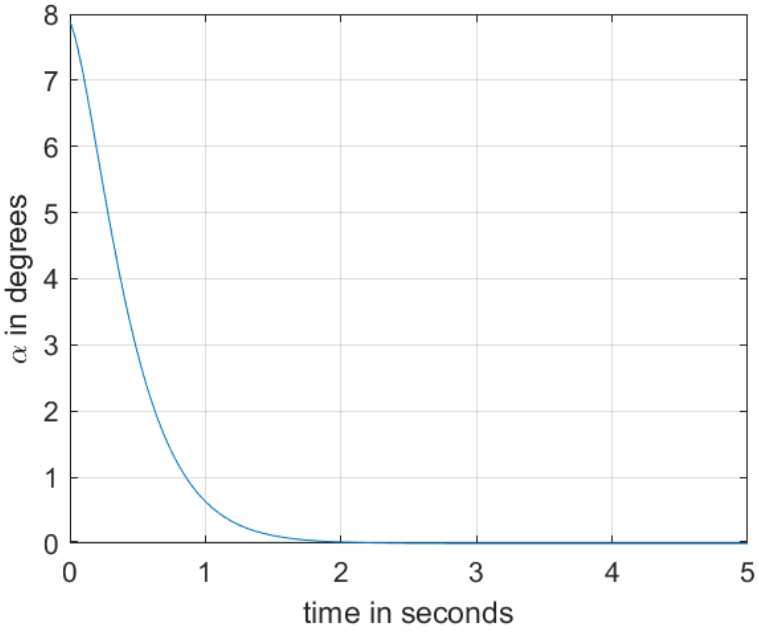

Figure 4.2: Value of α as the Platoon Drives Straight

Fig. 4.3 shows how Δl behaves as the vehicles turn in a circular arc. Although Δl is not driven entirely to zero during the time frame of the simulation, the magnitude of the final value of Δl in the simulation is less than 0.0005 meters, which means the tow bar was compressed less than half a millimeter, which still means that the controller still performed well. Fig. 4.4 shows how α was driven to zero during the simulation.

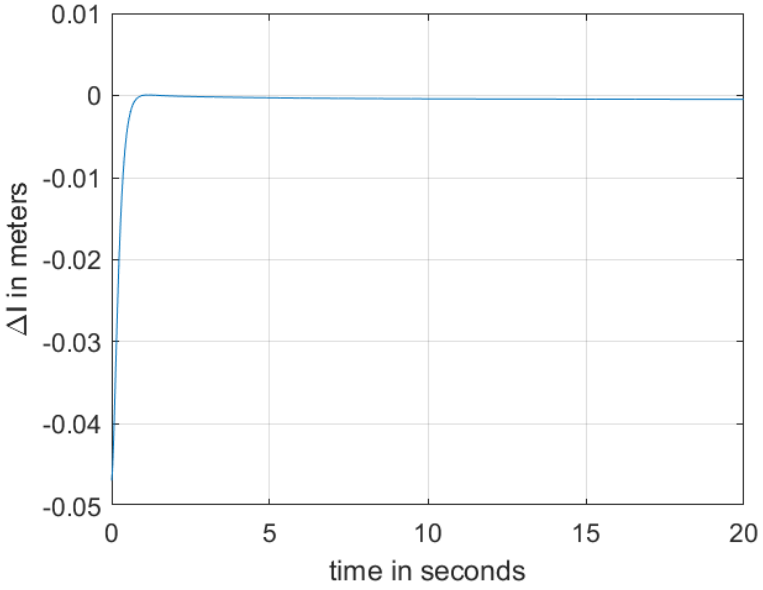

Figure 4.3: Value of Δl as the Platoon Turns

Although the controller was successful in driving α to zero, because the platoon was turning in a circular arc, the follower truck did not travel through exactly the same path that the leading truck. The lateral offset between the path of the follower truck and the path of the leader truck was about 1.19 meters during much of the turn. Fig. 4.5 shows a plot of the path of the hitch of each truck, as well as a drawing of where each truck was at the end of the simulation. The axes of the graph are in meters, and the origin is at the original position of the leading truck's hitch. This simulation was run for 20 seconds, so that the trucks would traverse a longer distance and make their paths easier to see.

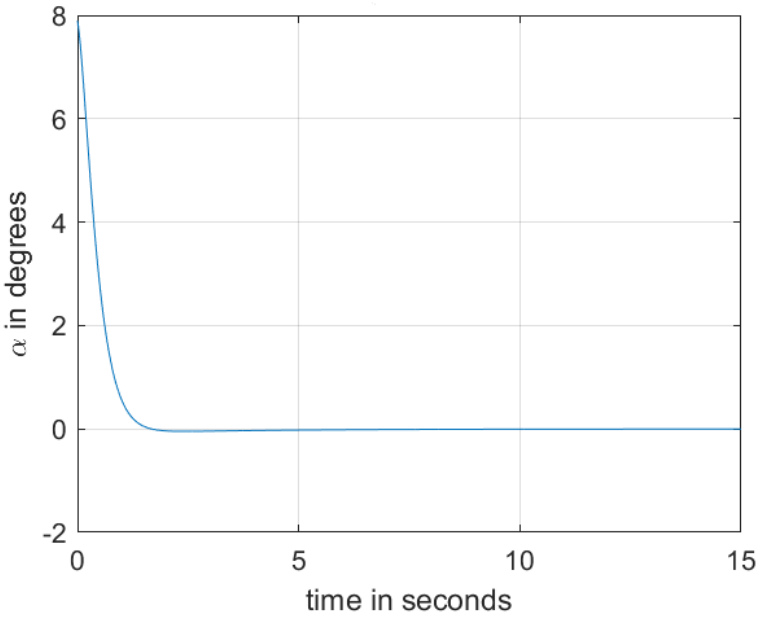

Figure 4.4: Value of α as the Platoon Turns

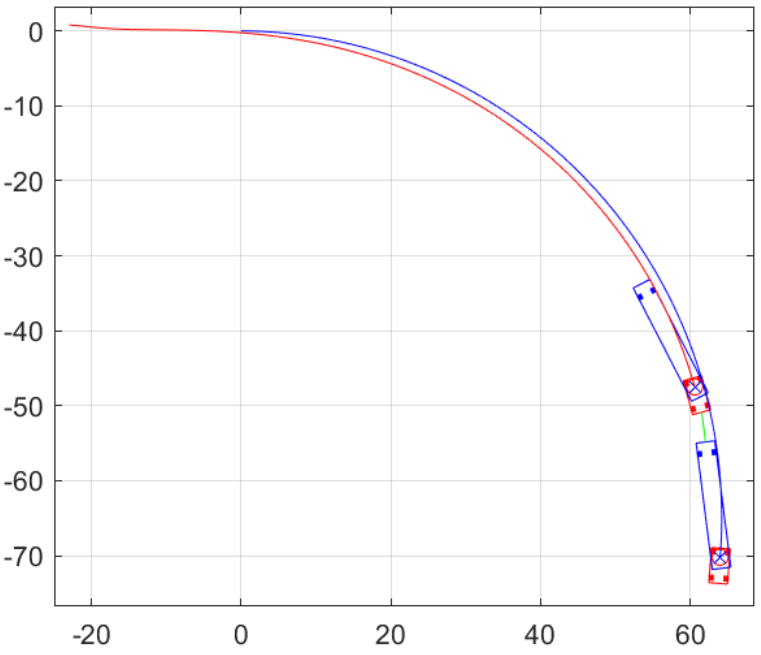

Figure 4.5: Paths of the Trucks as the Platoon Turns

This lateral error was likely caused by the specific choice of control objectives. As shown in the first simulation, minimizing α minimizes the lateral difference between the truck paths when the lead truck is driving in a straight line. However, when the lead truck drives in a circle, the articulation angle of the lead trailer is no longer zero, which means that the leading trailer may not be centered over the path traveled by the leading truck. If α is zero, then the follower truck will be directly behind the leading trailer, but the leading trailer might not be over the path of the leading truck.

An additional simulation was run in which the platoon made a double lane change. This particular test is important because it shows how the system might behave in a common real-world scenario. In this simulation, both trucks have an initial speed of 13 meters per second, and the lead truck maintains that speed. The following trailer has an initial articulation angle of -1.5 degrees, and the follower truck has an initial yaw angle of 3 degrees. The tow bar is initially stretched by 5.2 centimeters. The simulation was run for 19 seconds.

This simulation also investigated the controller's response to parameter uncertainties. The controller needs to know the value of many parameters of the system, such as the mass of the truck, the moment of inertia of the truck, the cornering stiffness of the tires, and so on. Although all these values are easily accessed in a simulation, some values may be hard to measure for real-world experiments. In particular, the moment of inertia of the truck, the moment of inertia of the trailer, and the cornering stiffness of the tires are thought to be the most difficult system parameters to measure. To see how the controller would react to parameter estimate errors in a real experiment, this simulation also included parameter estimation errors. Specifically, the controller overestimated the moments of inertia of the truck and trailer by 25% and underestimated the cornering stiffness of the tires by 25%.

Fig. 4.6 shows how Δl is driven towards zero by the controller. The term Δl shows a small disturbance when the lead vehicle changes lanes, but this disturbance is quickly eliminated by the controller.

Fig 4.7 shows how α is also driven to zero by the controller. It also shows how the disturbances

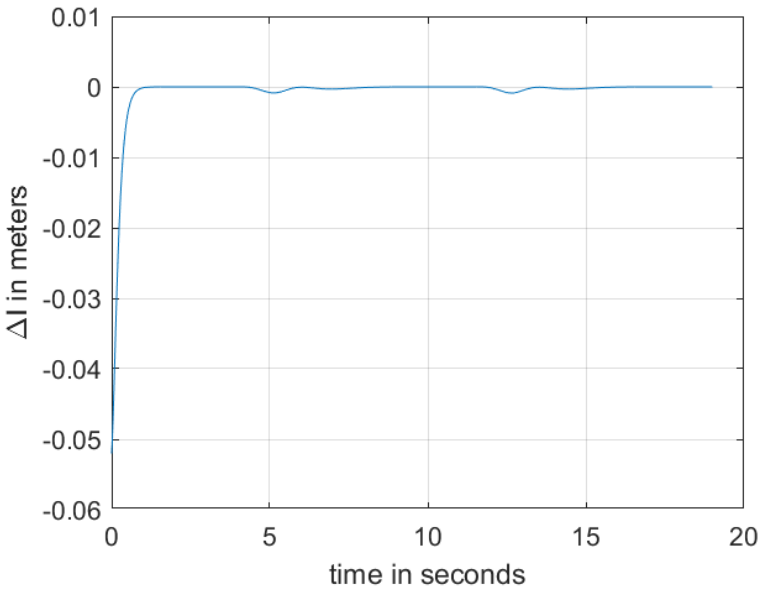

Figure 4.6: Value of Δl during a Double Lane Change

caused by the lane change are driven to zero.

The figure showing the entire trajectory of the trucks during the maneuver is very large, since the trucks were driving more quickly than in prior simulations, so the plot has been placed in Appendix B. Fig. 4.8 shows the trajectory of the trucks during the second lane change. The red line tracks the trajectory of the hitch of the lead truck and trailer while the blue line tracks the trajectory of the hitch of the following truck and trailer. Because of the dimensions of the figure, it is presented in landscape format. Fig. 4.8 shows that there is a small lateral tracking error during the lane change, but it is much smaller than the error during the simulation with constant turning and is quickly eliminated once the lane change is complete.

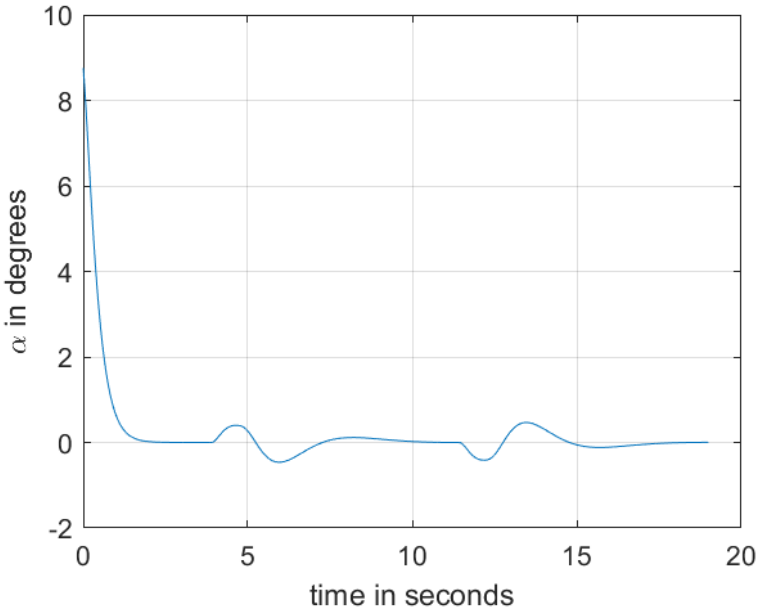

Figure 4.7: Value of α during a Double Lane Change

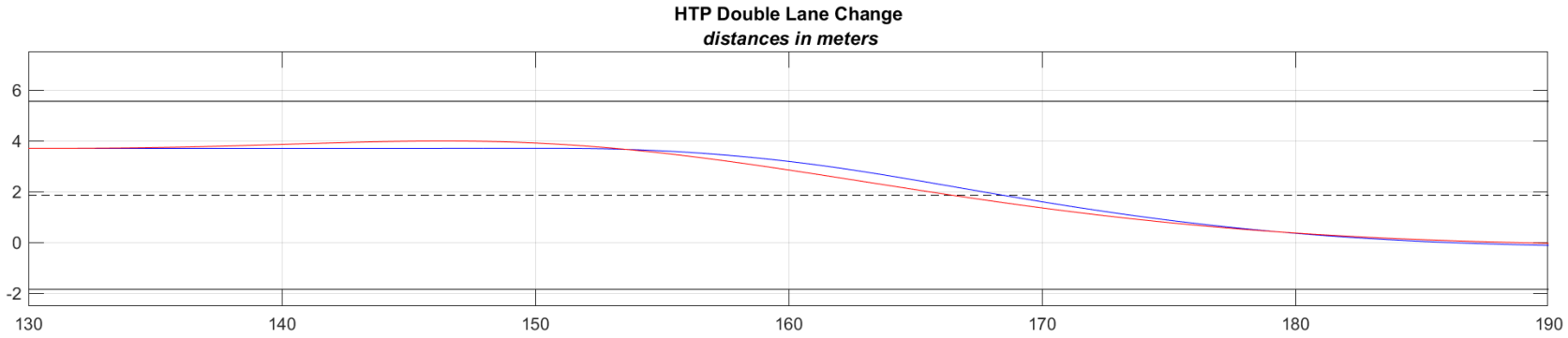

Figure 4.8: Detail of Trajectory of Platoon during a Double Lane Change

Another simulation was conducted to investigate the platoon's behavior during a U-turn, which is another common real-world scenario. The lead truck drove at a constant speed of 7 meters per second. The follower truck had an initial articulation angle of -2 degrees and an initial yaw angle of -1 degree. The initial value of Δl was about -6.8 centimeters, and the initial value of α was about -10 degrees. The same parameter errors from the double lane change simulation were used in this simulation as well.

Fig. 4.9 shows the value of Δl during the turn while Fig. 4.10 shows the value of α during the turn. Both plots show how the initial value of the outputs were driven toward zero by the controller. Both Δl and α have some small steady state error during the turn; Δl is about -3 millimeters, and α is about 0.7 degrees. When the lead truck straightens out after the turn, at about 13 seconds, there is a small disturbance in both outputs. However, the controller drives both toward zero as the turn is completed.

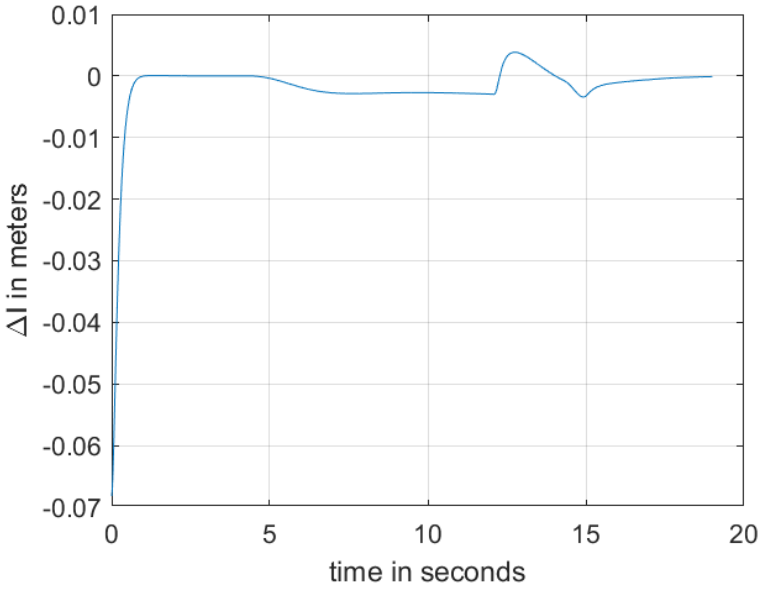

Figure 4.9: Value of Δl during a U-Turn

Fig. 4.11 shows the path that both trucks took during the U-Turn. There is some steady-state

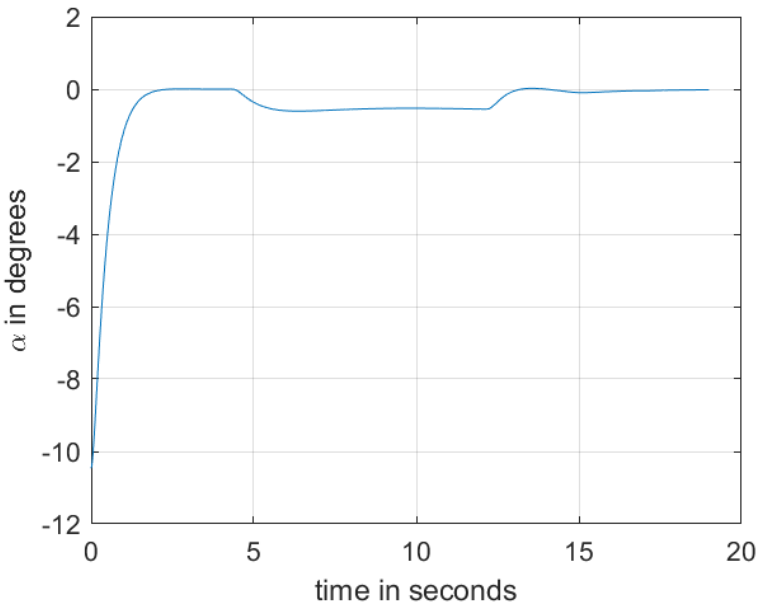

Figure 4.10: Value of α during a U-Turn

lateral tracking offset, just like there was in the previous turning simulation. In this simulation, the trucks were able to successfully navigate the U-turn even though it was very tight; the diameter of the circular path was about as long as the semi truck platoon itself. It should be noted that even though the turn had such a small diameter, the controller was able to keep α very small, at about 0.7 degrees.

Four different simulations have been run under different scenarios and under certain initial conditions. Overall, the controller drove the error towards zero, even in the presence of parameter uncertainties. although there was some lateral tracking error.

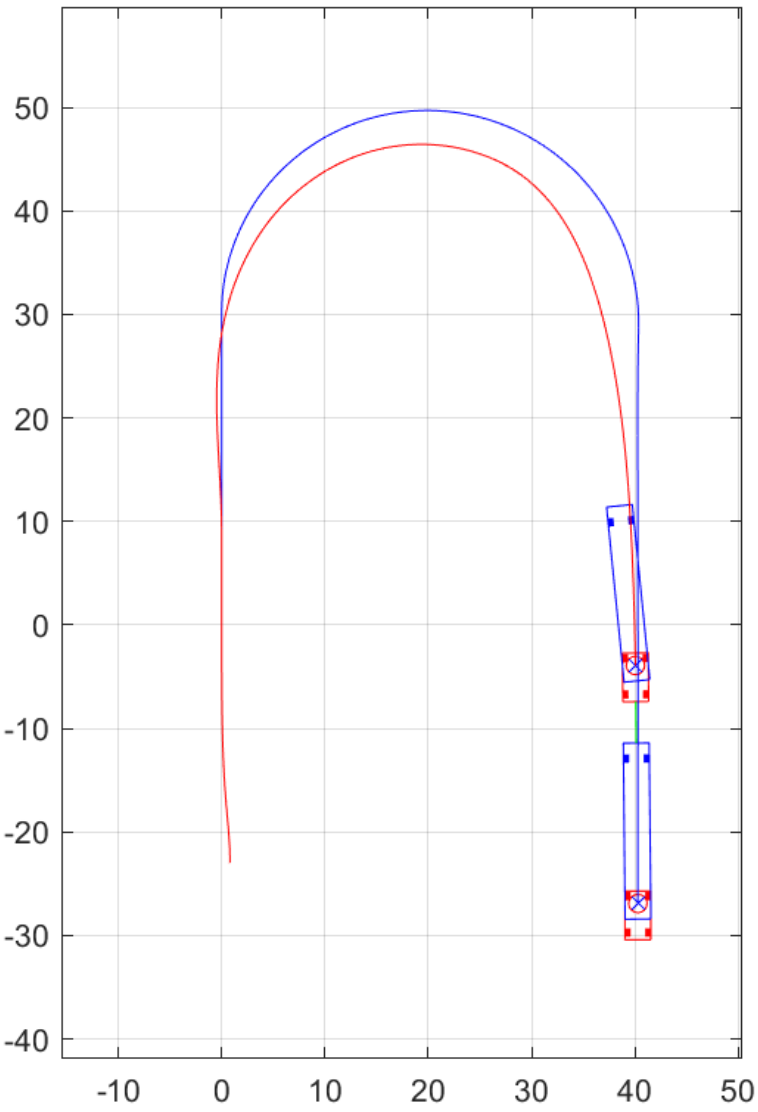

Figure 4.11: Paths of the Trucks during a U-Turn

5.1 Prototyping the Smart Tow Bar

As well as being tested in simulation, work is underway to implement HTP on full-size semi trucks. One semi truck and two semi trailers from TTI, the Texas A&M Transportation institute, have been procured, and Dr. Srikanth Saripalli's semi truck will also be borrowed for full-scale testing. Dr. Saripalli's truck is already drive-by-wire enabled through ROS, so it will be used as the following truck.

A mechanical engineering senior design team designed a prototype smart tow bar during the Spring 2019 semester and fabricated it with the help of the FEDC in the Summer 2019 semester. The prototype is shown in Fig. 5.1

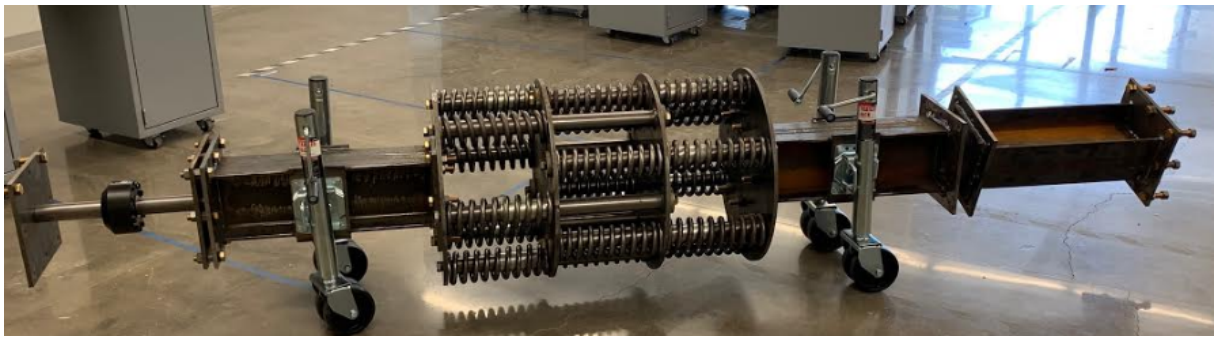

Figure 5.1: Picture of Prototype Tow Bar

The tow bar is made of bolted and welded steel. It was designed to withstand a compressive load of 13,000 pounds, which is the estimated load the tow bar would have to endure if the lead truck suddenly applied its brakes and the follower truck failed to respond, with a 1.5 factor of safety. The main structural element in the tow bar is a W8x24 I-beam that runs along the length of the tow bar. It has a turntable to allow for roll between the trucks as well as double pin joints at either end of the bar, to allow for pitch and yaw. The tow bar has a system of many springs to allow

for some compliance to reduce impact loads. The tow bar also features four wheels with adjustable heights, so that the tow bar can be easily moved to where it is needed. These wheels were part of an effort to make the tow bar only require a team of two people to operate. Additionally, Mike Ashley, a mechanical engineering senior, designed and fabricated steel mounts to connect the tow bar to the following truck and the leading trailer.

The spring system of the trailer has 18 springs which each have a spring constant of 675 pounds per inch and can be safely compressed by up to five inches. The springs are arranged into three sets of six parallel springs, separated by steel plates. One set of springs is compressed when the overall system is in tension, while the remaining two sets of springs are compressed when the overall system is compressed. This was chosen because the largest expected compression loads were greater and more safety-critical than the largest expected tensile loads. The combined system can compress up to ten inches and stretch up to five inches. It has a compressive spring coefficient of 2025 pounds per inch and a tensile spring coefficient of 4050 pounds per inch.

The tow bar also has two 13-bit encoders, one at each double pin joint, to measure the difference in yaw angle between each truck and the tow bar. The load cell is the tow bar is an SRP4-50K load cell rated for 50,000 pounds in compression and in tension. The load cell outputs an analog voltage signal proportional to the load on the load cell, while the encoders communicate using the Serial Synchronous Interface (SSI) protocol. An Arduino Mega as well as RS-422 line drivers and receivers have been procured to read data from these sensors, and work is underway to program the arduino. Once the signals have been read from the sensors, they will be sent to a nearby computer and logged using ROS.

5.2 Physical Experiment

On February 5th, the first full-scale experiment was conducted with the prototype smart tow bar at the RELLIS campus. For safety reasons, the experiment was very limited in scope; the lead truck would tow the following truck, at a very low speed (<5 miles per hour) while the following truck is in neutral. This was done as a first experiment to test if the tow bar would be strong enough for future testing. This test was conducted solely to determine the structural integrity and

performance of the tow bar, so no data was collected during the test.

Once the steel mounts were bolted to the leading trailer and the following truck, the double pin joints were bolted to those mounts. Then the trucks were driven into position and the tow bar was rolled to the trucks and bolted in place. In this experiment, the following truck was not hitched to a trailer of its own.

During the test, Drew Hubbard drove the lead truck, which was Dr. Saripalli's truck, and Mike Ashley drove the following truck. Both Drew and Mike have their CDL license. The author stood outside the vehicle to monitor the tow bar for any signs of bending or breaking. A three-way phone call was used to communicate during the experiment.

Once everyone was ready, Mike put the following truck in neutral and Drew gently accelerated the lead truck until reaching a speed of about 4 miles per hour. The tow bar showed no signed of damage, weakening, or deforming. Drew drove for a short distance and then coasted to a stop. Then Drew gently accelerated to about 4 miles per hour, made a gentle left turn (about 30 degrees in total) and then coasted to a stop. The tow bar's pin joints rotated as expected during the turn, and the tow bar showed no signs of damage. Then the experiment was finished and Mike and the author unbolted the tow bar from the trucks and returned it to its place in a nearby hangar.

The following figures show pictures taken from this first experiment. Fig. 5.2 shows the tow bar almost fully assembled. Fig. 5.3 shows the welded steel supports that Mike fabricated and bolted to the leading trailer, in order to reinforce its bumper to distribute the load applied to the bumper by the tow bar. Fig. 5.4 below shows the double pin joint bolted to the back of the leading trailer. Fig. 5.5 below shows a picture of the tow bar in its final assembled state, along with the author and Mike.

Figure 5.2: Prototype Tow Bar during Assembly

Figure 5.3: Welded Steel Supports Reinforcing the Bumper of the Leading Trailer

Figure 5.4: Double Pin Joint Bolted to Leading Trailer

Figure 5.5: Picture of Prototype Tow Bar

5.3 Commercialization

In addition to the technical work on this project, developed through deriving the dynamic model of the platoon, developing a nonlinear controller, implementing a simulation, and starting full-scale experiments, some work has also been done to investigate the commercialization opportunities for this technology.

Several ideas and applications for this technology were casually brainstormed over the course of this project, but to further this effort and explore outside perspectives, the team presented this project at the Texas A&M School of Innovation's Aggie Forum event on October 18th and 19th of last year.

The Aggie Forum is intended to allow project owners to present their project to interested members of the community, called participants, who help the project owners brainstorm solutions to problems and roadblocks in their project through a discussion managed by dedicated facilitators who are skilled in the best practices of creative brainstorming and innovation. These best practices include staying positive in everything one says, making one's thinking visible through the use of sticky notes, including everyone in a discussion, and focusing on generating a large number of ideas now and waiting to narrow down and refine ideas until later.

Mike, Dr. Gopalswamy, and the author were the owners of this project; professors from A&M, local businesspeople, faculty at the School of Innovation, and community members were participants; and Dr. Elizabeth Deuermeyer from the School of Innovation and Dr. Dennis Perkinson from TTI were the dedicated facilitators for this project.

The problems or roadblocks for this project were encapsulated in these four "activating questions." These questions do not necessarily convey the most difficult challenges on this project, but they were chosen because they would lead to the most valuable discussions with forum participants.

1. What are the barriers to public acceptance of autonomous vehicles?

2. How can these barriers by overcome?

3. What are the future applications of HTP?

4. Who or what would be the best market for HTP?

The participants thought of many, many ideas to answer these questions, and a full list of them is beyond the scope of this paper, but a few particularly interesting ideas will be noted here. Some of the major barriers to public acceptance of autonomous vehicles are that they are "scary" and not well understood by the public. To remedy these concerns, some participants thought that HTP should not be marketed as an autonomous vehicle technology at all. Because the lead driver is always in control of his vehicle, and the tow bar ensures the follower trucks follow though the same path, he is, in effect, controlling all the trucks in the platoon. Additionally, the lead truck can be thought of as actually towing the rest of the platoon, while the tow bars simply facilitate the platoon by controlling the throttle and steering of the following trucks to reduce some of the load on the lead truck. This idea seems appealing since people are much more comfortable and familiar with towing vehicles than they are with autonomous vehicles. To further this marketing strategy, HTP could be renamed or relabeled using terms like "long haul hitch," "truck bundling," "tandem long haul trucking," "convoy bar," and "tandem driving configuration."

Another interesting note addresses the concern that commercial truck drivers might be worried that HTP could eliminate some of their jobs. The idea is that HTP could be marketed as allowing each truck driver to haul more cargo than ever before, which is an appealing prospect to truck drivers since they are commonly paid based on the amount of cargo they transport.

Lastly, some participants thought that a good market for HTP could be the military. These participants thought that although the public may be wary to adopt this new technology, the military tends to be less risk-averse and would likely adopt it more readily. HTP could be useful in the military since the military commonly forms convoys of vehicles to transport soldiers, goods, and the vehicles themselves. HTP would allow the military to form convoys while requiring fewer solders to drive the vehicles. Finally, the public would be less concerned about using HTP if it has already been proven safe and reliable through years of use in the military. Commercializing this technology through the military could be easier than commercializing through private companies,

since Texas A&M already works on projects with the army at the RELLIS campus through the Army Futures Command.

6. CONCLUSION

6.1 Future Plans

This section summarizes future plans for this project. Immediate plans for implementing HTP include finishing programming the Arduino to read the data from the encoder and the load cell and then sending the data to a nearby computer which publishes the data to ROS. Once data can be read and recorded from the sensors on the tow bar, a series of more full scale tests will be conducted. The tests will start very small, like the first test, and gradually become more ambitious.

First, the initial full-scale test will be repeated while the data from the sensors on the tow bar is logged with ROS. This will be done to evaluate the data from the sensors to check if the quality of the data is sufficient for control.

Next, a simple controller, perhaps a proportional controller, will be written to control the steering of the following truck while the lead truck is driven slowly (5 miles per hour or less). In this test, the following truck would still be in neutral. This test would be conducted to verify that the control software works well with the data from the sensors. For safety reasons, the throttle control would not be tested in this initial experiment. A very simple controller would be used instead of a more advanced controller so that the system behaves predictably and the controller is easy to adjust during testing. For this first control test, Dr. Saripalli's semi truck will likely be used as the following truck since it is already drive-by-wire enabled through ROS.

The next test would be similar to the last one, but the throttle would be controlled instead of the steering. Next, the steering and throttle control would be combined. Completing this test with combined steering and throttle control would be regarded as a significant milestone in the project. After this test, basic system identification will be conducted on the following truck to better understand its dynamics, especially the engine dynamics. After this is completed, more advanced controllers will be written using this new information until the controller presented in this paper can be implemented on the full scale vehicles.

Additionally, the simulation of HTP will be expanded to test the controller under a wider variety of scenarios, especially when the system parameters are not well known. This would test the robustness of the controller. Engine dynamics, rolling resistance, and air drag would also be added to the simulation at this point. Other control objectives should be tested in simulation as well, especially control objectives that reduce the lateral tracking error shown by the current controller.

Alternative sensors would also be explored at some point during early full scale testing. Specifically, a camera will be mounted on the hood of the following semi truck and a computer vision system will be used to track the rotation at both pin joints as well as the contraction or expansion of the tow bar.

Before the controller presented in this paper can be implemented, a few more sensors need to be added to the tow bar system. Specifically, the articulation angle of the following trailer needs to be measured, and a similar computer vision system could be used to do this. Also, the acceleration and velocity of the following truck need to be measured, and this will probably be done using an INS system.

In the long-term, a new prototype tow bar should also be designed and fabricated to improve on the current prototype. A mechanical engineering senior design team could be used again in order to save on fabrication costs and to maintain some control and input on the design process. Detailed design requirements for the new tow bar are documented elsewhere, but the new tow bar ought to be lighter, weatherproof, easier to assemble, and able to have its length adjusted by hand. Using a hydraulic piston in the design is an appealing option, but the design process should be solution-neutral.

During later full-scale tests, the TTI truck ought to be used as the following vehicle so that Dr. Saripalli's truck will not have to be borrowed as often. The TTI truck is controlled using a dSPACE MicroAutoBox and dSPACE's proprietary software. This software can interface with Matlab, so that the truck can be controlled using Simulink. Additionally, Vamsi Vagamoor, a PhD student in the mechanical engineering department, has performed system identification on the TTI truck and has written a dynamic model of the truck using Dymolla. These software systems should all be

leveraged when the TTI truck is used as the following truck, although learning how to use them will require a significant time investment.

6.2 Technical Challenges

This section describes several potential obstacles that could prevent this project from being completed. Of course, there could always be more unforeseen problems with any major project, but these are a few of the main potential problems that come to mind.

The first main problem is that the automatic transmissions in the semi trucks acquired for this project (International ProStar Plus) change gears often, suddenly, and abruptly. When semi trucks change gears, the entire vehicle undergoes a large amount of jerk, which is vastly different from the behaviour of automatic transmissions in everyday passenger vehicles. These sudden changes in acceleration could potentially make the system very difficult to accurately control.

Another potential problem is the strength of the tow bar. If the welds on the prototype tow bar break during testing, it would likely take a long time to fabricate a replacement tow bar, which would significantly delay the project.

Another potential problem is that the lead semi trailer might not be able to withstand the tensile and compressive forces exerted by the tow bar.

Some parameters of the semi truck that were used in simulation, such as the cornering stiffness of the tires or the moment of inertia of the truck, can be difficult to measure. Although parameter uncertainty in these terms has been included in two of the simulations presented earlier, if the estimation errors are very large in a physical experiment, they could still make the system difficult to control.

To minimize the impact of these potential problems, the initial tests will be conducted at very low speeds (under 5 miles per hour), and future tests will gradually increase their speeds if these problems are not encountered.

6.3 Conclusion

This paper has shown a dynamic model of the semi truck platoon and a controller for the system based on feedback linearization. A simple simulation using Matlab and Simulink was made, and it showed that the controller succeeds in minimizing its control objectives, even in the presence of some parameter uncertainties, though the specific choice of control objectives leads to some lateral tracking error. A prototype tow bar was designed and fabricated. One full scale test was conducted, and more tests are planned. Finally, future plans and potential risks to the project completion were discussed.

REFERENCES

[1] A. Winder, "Study of the scope of intelligent transport systems for reducing co2 emissions and increasing safety of heavy goods vehicles, buses and coaches," tech. rep., ERTICO, September 2016.

[2] B. R. McAuliffe, M. Croken, M. Ahmadi-Baloutaki, and A. Raeesi, "Fuel-economy testing of a three-vehicle truck platooning system," tech. rep., National Research Council Canada, April 2017.

[3] B. Sheehan, F. Murphy, M. Mullins, and C. Ryan, "Connected and autonomous vehicles: A cyber-risk classification framework," *Transportation Research Part A: Policy and Practice*, vol. 124, pp. 523 – 536, 2019.

[4] R. McLane, "Platoonpro truck platooning safety report," tech. rep., Peloton, 2019.

[5] S. Gopalswamy, "Extreme hard platooning," tech. rep., Texas A&M University, August 2018. Texas A&M University Internal Disclosure of Invention.

[6] A. Mendes, A. Fleury, M. Ackermann, and F. Leonardi, "Heavy-duty truck platooning: A review," January 2017.

[7] T. Ogitsu, T. Ikegami, S. Kato, and H. Mizoguchi, "Study of coupling technologies for personal vehicle transit," in *2014 International Conference on Connected Vehicles and Expo (ICCVE)*, pp. 775–776, November 2014.

[8] ASI, "Asi guideline for autonomous convoy: Safe, simple, reliable." Web, May 2017. https://www.asirobots.com/asi-guideline-autonomous-convoy-safe-simple-reliable/.

[9] M. Barber, "Finally, a camper that could be towed by an electric car." Web, August 2018. https://www.curbed.com/2018/8/29/17795996/camper-trailer-electric-dethleffs.

[10] T. Ogitsu and M. Omae, “Design and experimental testing of vehicle-following control for small electric vehicles with communication,” in *2015 6th International Conference on Automation, Robotics and Applications (ICARA)*, pp. 586–590, February 2015.

[11] T. Ogitsu, T. Ikegami, S. Kato, and H. Mizoguchi, “Application of draw wire encoder to vehicle-following device for personal vehicle,” in *2014 IEEE International Conference on Vehicular Electronics and Safety*, pp. 50–54, December 2014.

[12] T. Ogitsu, T. Ikegami, S. Kato, and H. Mizoguchi, “Distributed driving system for coupled small ev using neural network and load cell,” in *2015 6th International Conference on Intelligent Systems, Modelling and Simulation*, pp. 34–39, February 2015.

[13] T. Ikegami, T. Ogitsu, and H. Mizoguchi, “Distributed power control evaluation of hard-link-type mobility using velocity and load data,” in *2015 International Conference on Connected Vehicles and Expo (ICCVE)*, pp. 362–366, October 2015.

[14] T. Ogitsu, “Design and simulation evaluation of distributed driving control for combination of personal vehicles,” in *2016 4th IIAE International Conference on Industrial Application Engineering*, pp. 463–466, January 2016.

[15] M. Gäfvert, M. Sanfridsson, and V. Claesson, *Truck Model for Yaw Dynamics Control*. Technical Reports TFRT-7588, Department of Automatic Control, Lund Institute of Technology (LTH), 2000.

[16] C. Chen and M. Tomizuka, “Modeling and control of articulated vehicles,” *Institute of Transportation Studies, UC Berkeley, Institute of Transportation Studies, Research Reports, Working Papers, Proceedings*, January 1997.

APPENDIX A

DYNAMICS DETAILS

The equations governing the dynamics of a semi truck and trailer were shown in section 2 only at a very high level, for the sake of brevity. They are discussed in this appendix in more detail for the interested reader. Some equations first presented in section 2 are printed again here for convenience.

The state vector of the system of a truck and trailer is shown below in Equation (A.1).

$$\vec{\zeta} = \left[U, V, r, \dot{\psi}, \psi, \theta, x, y\right]^{\top} \tag{A.1}$$

The equation of motion of the system is shown below in Equation (A.2)

$$M\left(\vec{\zeta}\right)\dot{\vec{\zeta}} = \vec{f}\left(\vec{\zeta}\right) \tag{A.2}$$

Equation (A.3) below shows the mass matrix $M(\vec{\zeta})$. For brevity, several abbreviations are used in the following equation. Here m_v and m_t stand for the mass of the truck and the mass of the trailer, respectively. The total mass of the truck and trailer, which is $m_v + m_t$, is expressed as m, q_1 stands for $m_t d_t \sin\psi$, and q_2 stands for $m_t d_t \cos\psi$.

$$M(\vec{\zeta}) = \begin{bmatrix} m & 0 & q_1 & q_1 & 0 & 0 & 0 & 0 \\ 0 & m & (m_v d_v - q_2) & -q_2 & 0 & 0 & 0 & 0 \\ 0 & m_v d_v & I_v & 0 & 0 & 0 & 0 & 0 \\ q_1 & -q_2 & I_t & I_t & 0 & 0 & 0 & 0 \\ 0 & 0 & 0 & 0 & 1 & 0 & 0 & 0 \\ 0 & 0 & 0 & 0 & 0 & 1 & 0 & 0 \\ 0 & 0 & 0 & 0 & 0 & 0 & 1 & 0 \\ 0 & 0 & 0 & 0 & 0 & 0 & 0 & 1 \end{bmatrix} \tag{A.3}$$

Equation (A.4) below shows the forcing function $\vec{f}(\vec{\zeta})$. In this equation, $\bar{X}_1$ and $\bar{X}_2$ are the sum of the longitudinal tire forces acting on the truck and on the trailer, respectively, $\bar{Y}_1$ and $\bar{Y}_2$ are the sum of the lateral tire forces acting on the truck and on the trailer, and $\bar{Z}_1$ and $\bar{Z}_2$ are the sum of the torques acting on the truck and trailer due to the tire forces. If aerodynamic forces or rolling resistance were included in this model, they could be summed into these terms.

$$
\begin{aligned}
F_1 = mr_vV_v - m_td_t\left(\dot{\psi}+r_v\right)^2\cos(\psi)+ \\
m_vr_v^2d_v + \bar{X}_v + \bar{X}_t\cos\psi - \bar{Y}_t\sin\psi \\
F_2 = -mU_vr_v - m_td_t\left(\dot{\psi}+r_v\right)^2\sin\psi+ \\
\bar{Y}_v + \bar{X}_t\sin\psi + \bar{Y}_t\cos\psi
\end{aligned}
$$

$$
\vec{f}(\vec{\zeta}) = \begin{bmatrix}
F_1 \\
F_2 \\
-m_vd_vU_vr_v + \bar{Z}_v \\
m_td_tr_v\left(U_v\cos\psi + V_v\sin\psi\right) + \bar{Z}_t \\
\dot{\psi} \\
r \\
U\cos\theta - V\sin\theta \\
-U\sin\theta - V\cos\theta
\end{bmatrix} \tag{A.4}
$$

The control system shown in this paper requires the mass matrix $M(\vec{\zeta})$ to be invertible. The description below explains why $M(\vec{\zeta})$ is indeed invertible.

The determinant of $M(\vec{\zeta})$ is shown below in Equation (A.5).

$$
\det M\left(\vec{\zeta}\right) = I_vI_tm^2 - I_tmm_v^2d_v^2 - I_vmm_t^2d_t^2 + m_v^2m_t^2d_v^2d_t^2\left(\sin\psi\right)^2 \tag{A.5}
$$

However, I_v and I_t are the moments of inertia of the truck and trailer about their hitches, not their centers of mass, so these terms can be broken down further using the parallel axis theorem, as shown below in Equation (A.6), where I_{cmv} and I_{cmt} are the moments of inertia of the truck and trailer about their centers of mass.

$$\begin{aligned} I_v &= I_{cmv} + m_v d_v^2 \\ I_t &= I_{cmt} + m_t d_t^2 \end{aligned} \tag{A.6}$$

Substituting Equation (A.6) into Equation (A.5) and simplifying produces Equation (A.7).

$$\det M(\vec{\zeta}) = m^2 I_{cmv} I_{cmt} + m m_v m_t \left(d_t^2 I_{cmv} + d_v^2 I_{cmt} \right) + \left(m_v m_t d_v d_t \sin\psi \right)^2 \tag{A.7}$$

All three terms in the determinant are positive, and the first two terms are nonzero, so the determinant cannot be zero, so the matrix must be invertible.

APPENDIX B

FIGURE OF DOUBLE LANE CHANGE

Fig. B.1 shows the entire trajectory of both trucks during the double lane change simulation. The red line tracks the trajectory of the hitch of the lead truck and trailer, while the blue line tracks the trajectory of the following truck and trailer. Because of the dimensions of the figure, it is presented in a landscape orientation.

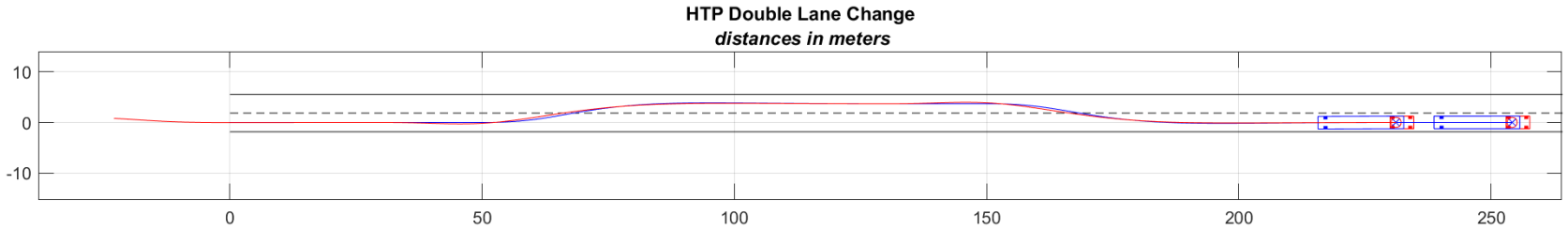

Figure B.1: Complete Trajectory during a Double Lane Change